Bachelor's Thesis

Forces in Soft Particles

prepared by

Markus Richter

from Hildesheim

at the Max-Planck-Institute for Dynamics and Self-Organisation

Thesis period:	1st April 2014 until 8th July 2014
First Referee:	Dr. Matthias Schröter
Second Referee:	Prof. Dr. Sarah Köster

Abstract

In this thesis we describe the behaviour of a hydrogel under compression as an example for the mechanical characteristics of soft particles. For this purpose we use a setup consisting of two pistons to compress a single hydrogel sphere. We will analyse the various effects which appear in such measurements. In addition we will prove that the compression of our model bodies can be described with Hertzian theory for two magnitudes of the applied force. We will also give another example for a material which could be used for further measurements in this topic.

Contents

1 Introduction

In biophysics it has been discovered that biological materials can appear in many forms. One of these forms is the form of an elastic solid state body. Soft Matter physics is trying to give a deeper understanding of these materials. Important types of these materials are polymers, colloids, surfactants and liquid crystals. Well-known examples for these materials are rubber (polymer), milk (colloid), soap (surfactant) and display devices (liquid crystals).
In this thesis we want to have a closer look at the behaviour of soft matter usable in granular packings. For this purpose we take a look at the compression of polymer and gel bodies. Back in 1882 Hertz proposed a theory of the forces of two solid bodies in contact (see [1]). We want to apply this theory on measurements of the compression of single particles. As Materials we use polyacrylamide as an example for a gel and polydimethylsiloxane as an example for cross-linked polymer. Especially polyacrylamide is a material used in different research projects. Because of its special characteristics it is adaptable to a lot of different requirements. Examples for research projects based on this material are the analysis of flows around elastic objects with PIV (see [2]) or the measurement of packing-fraction in packings of elastic spheres (see [3]). However PDMS is mostly known as a material used for building microchannels for experiments in microfluidics.
This thesis is divided into 5 chapters. The second chapter presents the background knowledge to describe the experiments. The experiments and the materials are then presented in chapter 3 and the results of our experiments follow in chapter 4. Finally we give a conclusion of our project and an outlook of what can follow these experiments.

2 Background

2.1 The characteristics of polymers

As both our materials are polymers we want to give a short description of the characteristics of polymers (see also [4]). Polymers are chain-like (macro-)molecules. They can be melted and then formed into a given shape. When curing they build a network to form a viscoelastic body. This means they recover their shape from deformations under small and short forces but deform irreversible over longer time or under larger forces. If the network has cross-linkers which connect the molecules the network is more stable and does not flow, but still has the ability to recover its form. Examples for cross-linked polymers are rubber or polydimethylsiloxan (PDMS). A special type of polymers are gels. They are made out of a mixture of a polymer network and a solvent. If this solvent is water they are called hydrogels. When the dry polymer is put into a corresponding solvent it will swell by absorbing the solvent. Likewise wet gel will shrink when exposed to air because the solvent evaporates. Examples for gels are polyacrylamide with water as a solvent and PDMS with organic solvents [5].

2.2 Hertzian compression

The Hertzian theory describes the forces of the contact of two solid bodies under the following conditions [6]:

- The significant dimension of the contact area a is small compared to the radius of the curvature of the body R.
- The strains are small (which results also in the assumption that $a \ll R$).
- Both solids can be considered as an elastic half-space.
- The surface is frictionless.

The main influences on the equations originate from the geometry of the problem. Besides there is the question which of our surfaces can be considered elastic and which one cannot. The curvature of the surfaces is the main variable of interest for this problem.

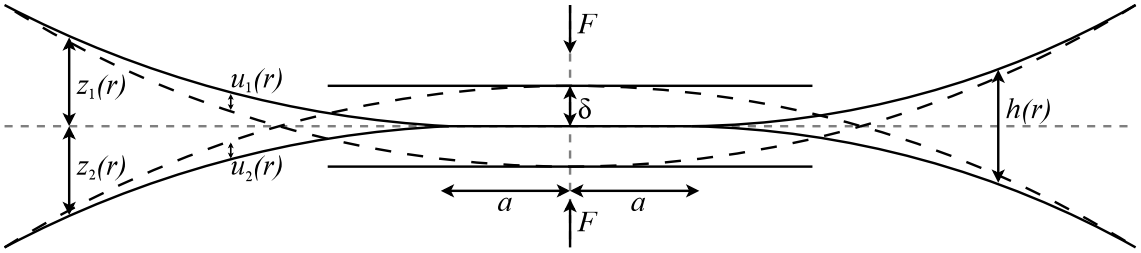

Figure 2.1: Compression of two elastic bodies with a convex surface.

In general we can start with a function of the distance of two surfaces h. Assuming we are close to the origin we can say that h is given approximately as

$$h(x, y) = Ax^2 + By^2 + Cxy \tag{2.1}$$

With this assumption the height z of the single surfaces of object 1 and 2 can be described as:

$$z_{1,2}(x, y) = \frac{1}{2R'_{1,2}}x^2 + \frac{1}{2R''_{1,2}}y^2, \tag{2.2}$$

with the two principal radii of curvature R' and R''. With these equations we get h as a function of the radii of curvature of the surfaces. We define R' and R'' as the principal relative radii of curvature and by suitable choices of axis we receive that $C = 0$. It follows:

$$h(x, y) = Ax^2 + By^2 = \frac{1}{2R'}x^2 + \frac{1}{2R''}y^2 \tag{2.3}$$

Now for solids of revolution with convex surfaces we can get $R'_{1,2} = R''_{1,2} = R_{1,2}$. It follows $A = B = \frac{1}{2}(1/R_1 + 1/R_2) =: 1/(2R)$.
Considering that the surfaces are able to deform we can describe the displacement of the single surfaces $u_{1,2}$ as:

$$u_1(x, y) + u_2(x, y) + h(x, y) = \delta, \tag{2.4}$$

with the total compression δ. With $x^2 + y^2 = r^2$ we get:

$$u_1(r) + u_2(r) = \delta - \frac{r^2}{2R} \tag{2.5}$$

For the pressure distribution p and the displacement u for solids of revolution according to [6] the following formulae apply:

$$p(r) = p_0\sqrt{1 - (r/a)^2} \tag{2.6}$$

and

$$u_{1,2}(r) = \frac{(1 - (\nu_{1,2})^2)}{E_{1,2}}\frac{\pi p_0}{4a}(2a^2 - r^2), \tag{2.7}$$

with r smaller or equal to the radius of the contact area a. Also ν is defined as the Poisson's ratio and E as the elastic modulus. We define $\frac{1}{E'} := \frac{1-\nu_1^2}{E_1} + \frac{1-\nu_2^2}{E_2}$ and together with equation 2.5 we get the following:

$$\frac{\pi p_0}{4aE'}(2a^2 - r^2) = \delta - \frac{r^2}{2R} \tag{2.8}$$

From this we receive $a = \pi p_0 R/2E'$ and $\delta = \pi a p_0/2E'$. The applied force is given by the integral over the pressure:

$$F = \int_0^a p(r)2\pi r \mathrm{d}r = \frac{2}{3}p_0\pi a^2 \tag{2.9}$$

Combining these we obtain:

$$\delta = \sqrt[3]{\frac{9F^2}{16R(E')^2}}, \tag{2.10}$$

The geometry of our problem poses an elastic sphere ($R_1 = d/2$) with a diameter d on an inelastic flat surface ($R_2 \to \infty$, $E_2 \to \infty$). We obtain:

$$\delta = \sqrt[3]{\frac{9F^2\left(1 - \nu_1^2\right)^2}{8dE_1^2}}, \tag{2.11}$$

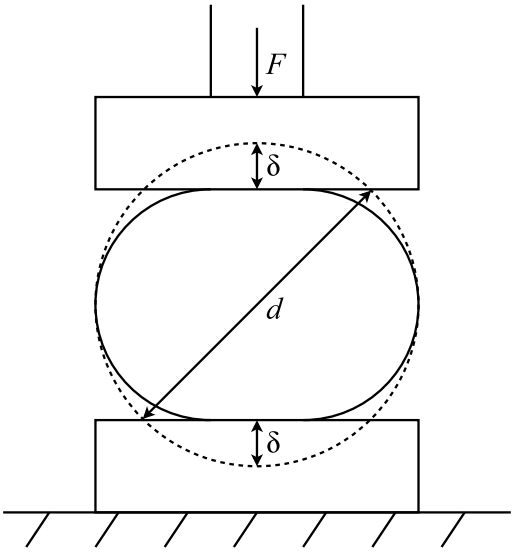

Figure 2.2: Compression δ of an elastic sphere with diameter d between two inelastic pistons with a force F. This geometry corresponds to the problem given in our setup.

2.3 Capillary bridges

One of the main effects influencing our experiments is the building of capillary bridges. Wet gels always have a liquid film on them when they are surrounded by air. When two surfaces are very close or even touch and at least one is wet, a capillary bridge builds up between them creating an attractive force. This force can be described by the Young-Laplace equation[7]:

$$\Delta P = \gamma \left(\frac{1}{r_1} - \frac{1}{r_2} \right), \tag{2.12}$$

whereby ΔP is the pressure difference between two liquid faces, γ is the surface tension of the liquid and r_1 and r_2 are the principal radii of curvature of the interface. The resulting force between the hydrogel sphere and the flat piston can be described by[7]:

$$F = 2\pi R_1 \left(\cos(\theta_1 + \beta) + \cos(\theta_2) - \frac{D}{r} \right), \tag{2.13}$$

with the sphere radius R_1, the contact angles $\theta_{1,2}$, the distance between the sphere and the surface D and curvature radius of the liquid-vapour interface r. As we didn't calculate the capillary forces in detail in this thesis we recommend to look for further details about this in the literature.

3 Materials and Methods

3.1 Materials

3.1.1 Hydrogels

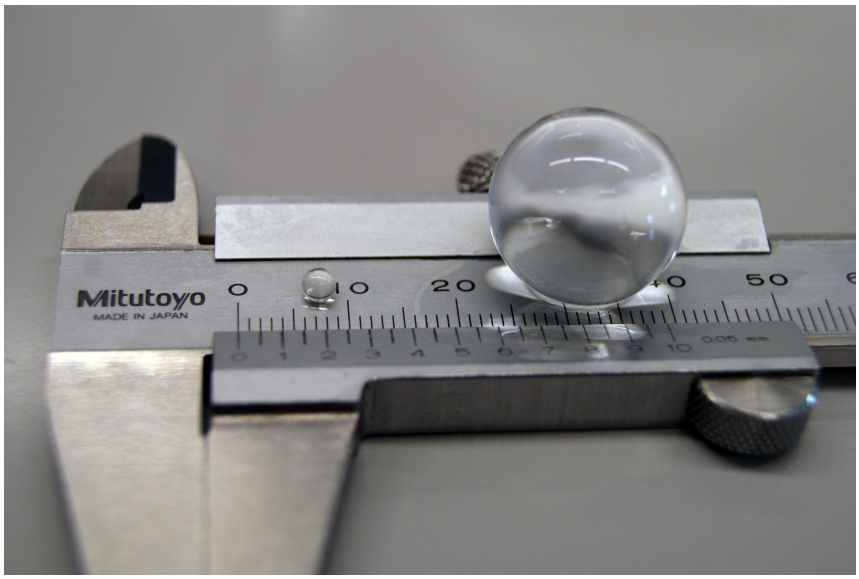

Figure 3.1: Hydrogel spheres used for our measurements. On the left hand side in dry state (ca. 3 mm in diameter) and on the right hand side in the wet state (ca. 18 mm in diameter).

The first particles we use in our experiments are hydrogel spheres[1]. You can see them in figure 3.1. These are made of polyacrylamide and can absorb large amounts of water. In the dry state the spheres are about 3 mm in diameter. When put into water they grow in a few hours to a diameter of ca. 18 mm. This results in roughly 216 times the volume of the sphere in dry state. Because of this property this material is also called super absorbent.

[1] As they are not made by ourself but bought from a company we also call them Aqualinos or GB710. For our measurements we use GB710 if not otherwise declared

In the wet state the particles have certain special characteristics which make them interesting for scientific purposes:

- The particles are nearly frictionless.
- They are transparent and have nearly the same refraction index as water (which makes them almost invisible under water).
- They have nearly the same density as water (which makes them buoyant).
- They can be formed in a desired shape and filled with tracer particles.

Therefore they are a good material to measure forces inside particles in granular packings. For our experiments we only use single spheres grown in pure water. It is also possible to grow them in salt-water. Although they only grow to smaller sizes the more salt you add to the water[2]. They can be stored for months in the water without change, but over longer times biofilms starts to grow on the surface of the particles. For precise measurements it is recommended not to store them more than a few weeks.

3.1.2 Polydimethylsiloxane (PDMS)

The second material we use in this thesis is polydimethylsiloxan, also known as PDMS. PDMS is a quite common material for example to build microfluidic channel structures. The material is made from viscous silicon elastomer and liquid silicon elastomer curing agent in the lab. As we want to use them for measurements of the strain field in a circular disc we create a layer of bronze particles which have a size of roughly $70\,\mu$m inside the discs. The bronze particles serve as tracers for the displacements inside the discs.
For the production we need moulds of the desired shape and the following amounts of material:

material	amount (relative)
silicon elastomer	100
curing agent	10
bronce particles	1

[2]This works of course only until a critical salt concentration is reached.

First we mix half of the needed silicon elastomer and curing agent and put it into a vacuum chamber for half an hour to remove the air-bubbles. Then we pour it into the moulds of the desired shape until they are a bit more than half filled. In our case we have used a PVC mould with circular holes of 15 mm diameter and 9 mm depth. This can be seen in figure 3.2. The PVC material helps to get the PDMS out of the moulds again as it is quite sticky on most surfaces.

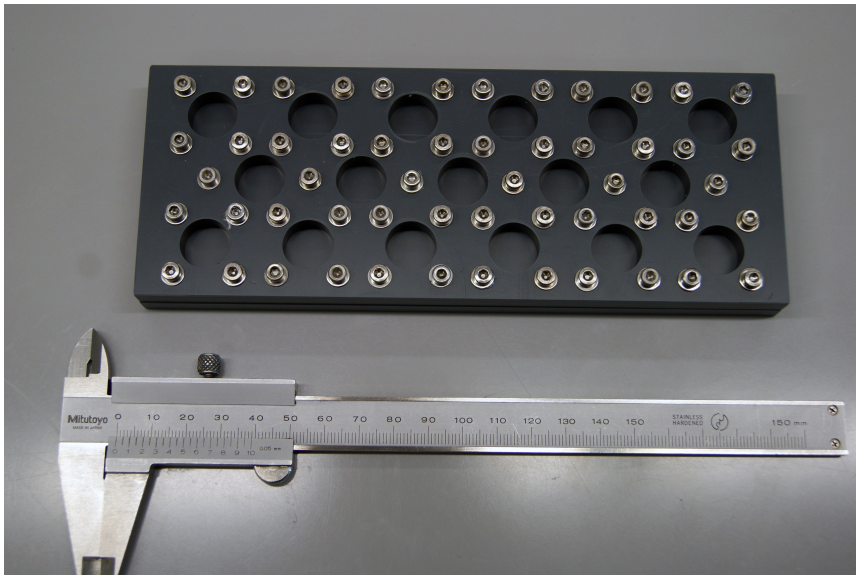

Figure 3.2: Moulds used for the PDMS production. The holes are 9 mm deep and have a diameter of 15 mm. The backplate can be removed so the discs can be removed quite easily from the moulds.

After that we wait for the next day before we continue with the second part. During this time the material cures to its final state. As a side effect it will shrink a little and might get a curved surface in the moulds. This happens as the material dries faster on the outside than on the inside. Therefore it contracts more in the middle than on the outside.
For the second part we mix the second half of the silicon elastomer and the curing agent with the bronze particles and put the mixture into the vacuum chamber for an hour as well. After that we pour the second mixture in the moulds over the ones previously made. The bronze particles will sink into a layer at the bottom of the second batch as they have a higher density than the PDMS material. Now the material needs time to dry again.
When the second part has cured too, the discs can be removed from the moulds and stored for later usage. In our case we disassemble the ground plates from our

moulds and push the discs out of the holes. As mentioned before the discs are quite sticky and have to be remove with a gently applied force. The resulting discs are shown in figure 3.3.

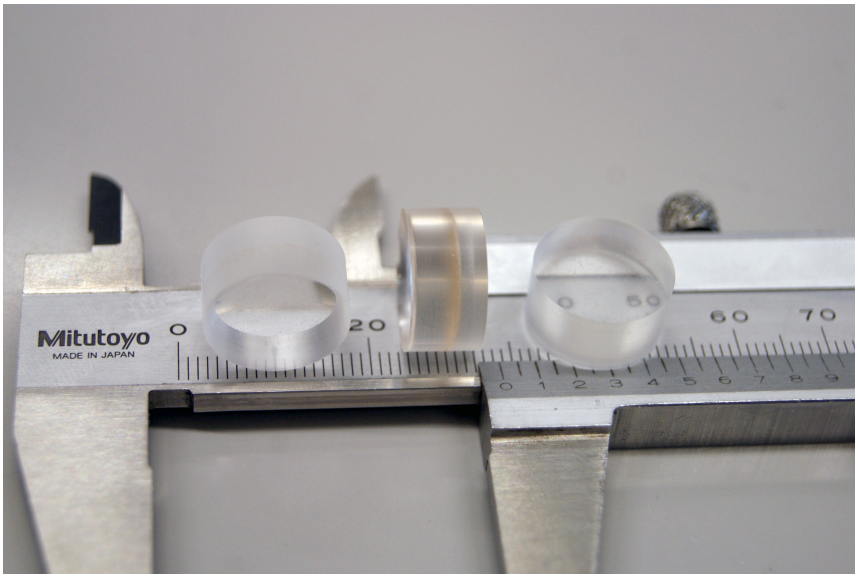

Figure 3.3: PDMS discs with a bronze layer in them. The discs have a diameter of 15 mm and a height of 9 mm.

3.2 The sphere compression setup

The sphere compression setup was developed during my employment at the institute prior to this thesis. It is able to measure the compression of a particle on a certain force. To accomplish this the particle of interest is put between two pistons (see figure 3.4). The piston on the top is connected to a stepper motor and the piston on the bottom is positioned on a scale. The applied force F can be calculated from the measured weight by the well known equation $F = m \cdot g$. In our case m is the measured weight and $g = 9.81 \frac{\mathrm{m}}{\mathrm{s}^2}$ the gravitational acceleration. The compression δ can be calculated from the distance of the two pistons measured by a laser distance sensor attached to the top piston. The Setup can be controlled via a Labview program. An important detail to keep in mind is that the sphere is compressed from both sides (top and bottom). Therefore the actual compression δ is only half the absolute distance change of the top piston. The piston on the bottom is slightly curved to help keeping the sphere between the pistons (curvature radius 750 mm)

and the pistons are in a glass tube to reduce evaporation. As the curvature radius is much larger then the sphere size we consider the bottom piston as flat too. The bottom piston is always made of steel whereas the material of the top piston can be changed or other surfaces like leafs can be attached to it.

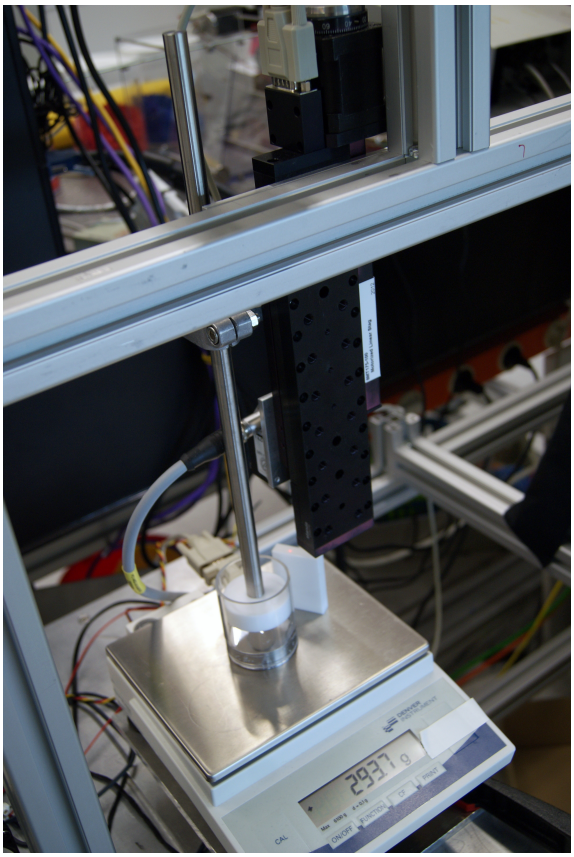

(a) The whole Setup.

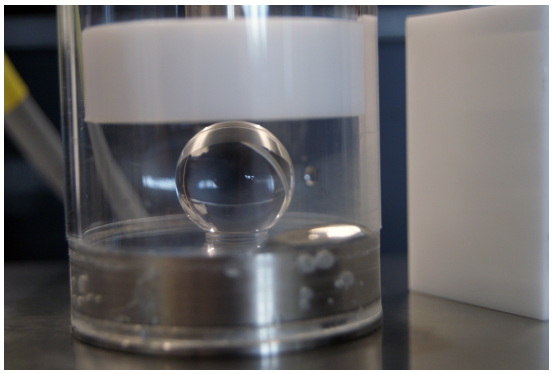

(b) Detailed view of the glass cylinder.

Figure 3.4: The sphere compression setup. A hydrogel sphere is compressed between two pistons in a glass cylinder. The top piston and a laser distance sensor are attached to a translation stage. The bottom piston lies on a scale which measures the applied weight and therefore the force.

One of the problems we encountered during our work was the building of a capillary bridge between the wet hydrogel sphere and the top piston. In our measurements this is visible as a negative force applied on the sphere. This negative force represents the attracting capillary force. This makes it difficult to estimate the force near the contact point of the sphere and the top piston. Therefore we tried different methods to reduce this effect.
First of all we use polished steel and a teflon top piston. The teflon piston is more

hydrophobic than the metal piston. We also made tests with several other hydrophobic surfaces on the top piston. These were Parafilm[3], wrapping film, sunflower oil and fluorinated oil. The effect of these surfaces is shown in figure 3.5. The solid materials reduce the effect of the capillary bridge compared to the metal piston. The oils don't seem to have much of an effect. Furthermore they have the problem of the application of the liquid before each measurement.

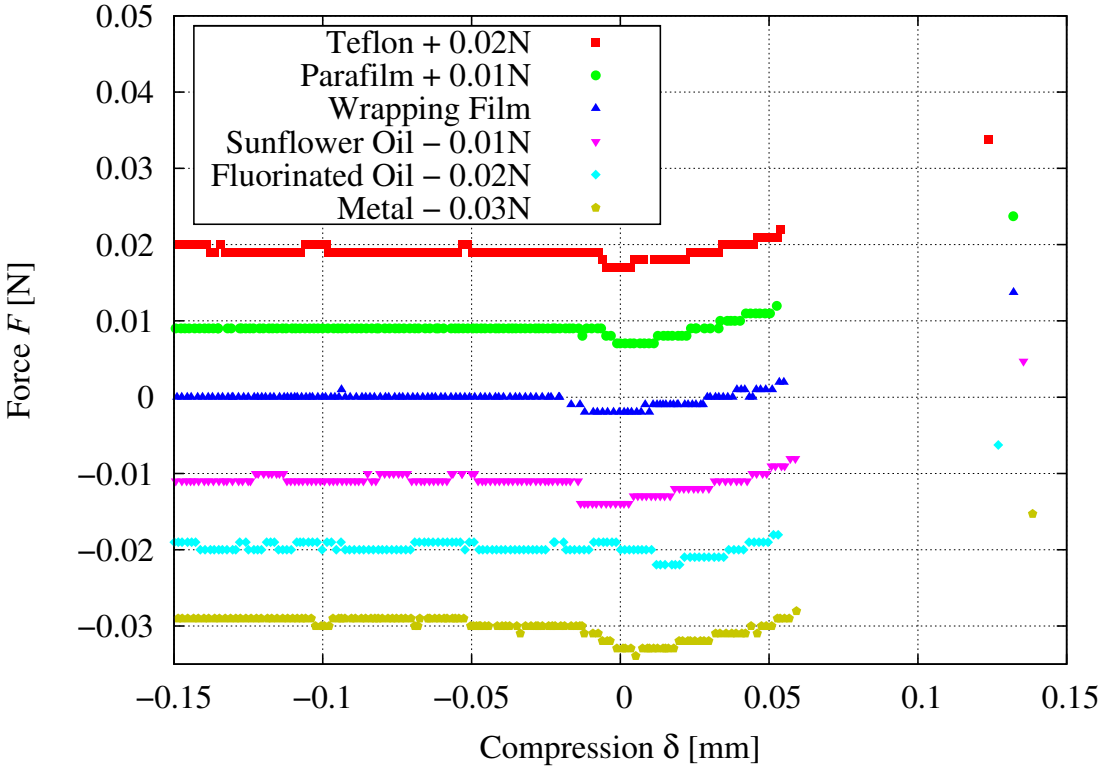

Figure 3.5: The effect of different top piston surfaces on the force F. At the point of contact a negative force is visible. This is caused by the building of a capillary bridge between the top piston and the wet hydrogel sphere. The lower amount of data points on the right side is caused by the measurement algorithm.

Moreover we tried the addition of a surfactant to the water the hydrogels are grown in. For that we used sodium dodecyl sulfate (SDS) as a surfactant. These measurements can be seen in figure 3.6. The SDS has an effect on the measurement when a metal piston is used, but almost no effect on the measurement with the teflon piston. Besides a surfactant adds the problem of the control over its concentration to the process.

[3]A film used for sealing bottles

Additionally we did a measurement with a completely water filled cylinder. This is depicted in figure 3.6. The measurement seems to solve the problem with the capillary bridge but causes another problem. Beside the fact that the evaporation is highly increased (compare figure 3.8) the buoyant force of the top piston has to be calculated for each position change. For this the height of the piston in the water has to be well known for every data point.

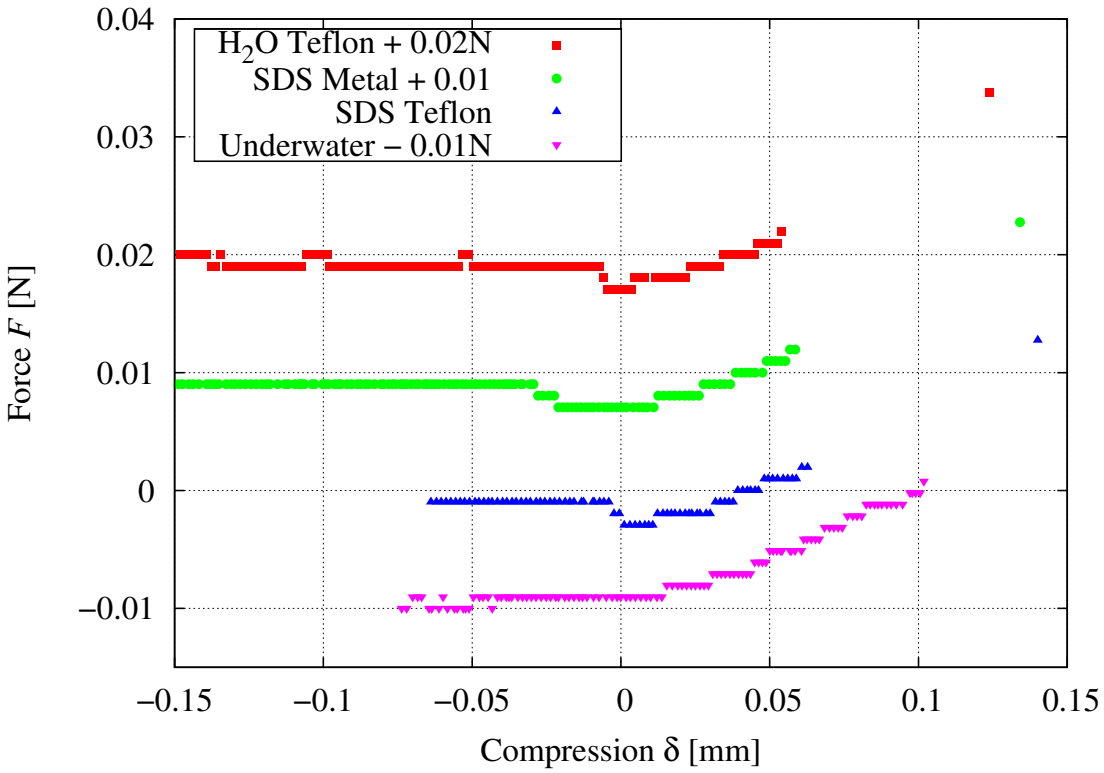

Figure 3.6: Effects of surfactant (SDS) in the hydrogels and measurements with a water filled cylinder (underwater) compared to pure water grown hydrogels in air. The building of the capillary bridges can be seen for the measurements in air. With a water filled cylinder the capillary bridge building is suppressed but buoyant forces become a severe problem. The lower amount of data points on the right side is caused by the measurement algorithm.

Last we made several tests with super-hydrophobic leaves provided by the Botanical Garden in Göttingen. The leaves we used are from fustet, nasturtium and lotus. The effect, also known as lotus-effect, completely prevents the building of a capillary bridge to the top piston within the resolution of the scale. This can be seen in figure 3.7. However the mechanical properties of the leaves themselves are unknown and change the resulting forces.

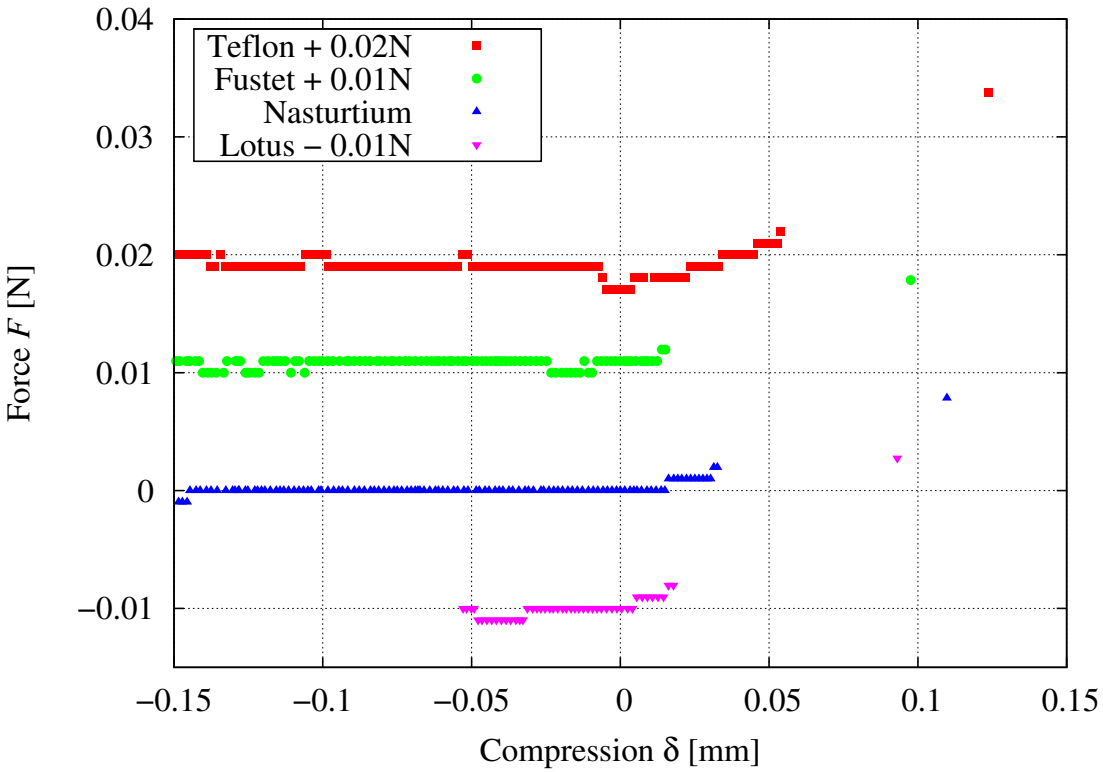

Figure 3.7: The effect of leaves attached to the top piston on the measurements. The capillary bridges are suppressed but the mechanical properties of the leaves have to be calculated. The lower amount of data points on the right side is caused by the measurement algorithm.

In the end we used a teflon piston with hydrogels grown in pure water. We abandoned the other ideas as the effects on the measurements are harder to estimate than the capillary bridges. For the measurements as presented in chapter 3.2.1 we assume the capillary force as constant over the whole time after the first contact is made (visible by the rising force after the jump to a negative force in the measurement). For this purpose we add the maximum negative force, measured at the beginning of each experiment, to all data points.
Another important effect we want to look at is the evaporation during the experiments. The evaporation in an uncompressed state is depicted in figure 3.8. As you can see a noteworthy evaporation only takes place in the water filled cylinder. The variations in the data can be explained by the fact that the experiment was standing in a room with some activity by people around it for several days. Possibly there also were small temperature and humidity changes in that time.

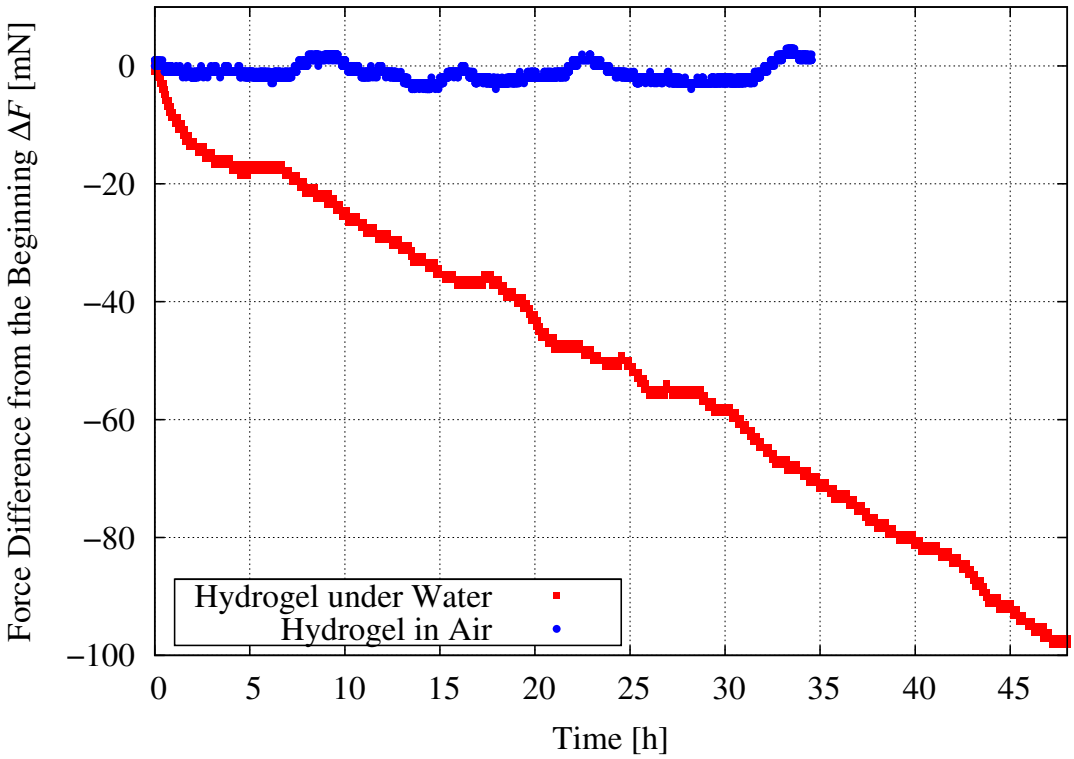

Figure 3.8: Change of the force compared to the measured force at beginning ΔF over time caused by the evaporation of the water. Hydrogel under water means that we use a water filled cylinder and hydrogel in air means a hydrogel sphere in the setup surrounded by the otherwise empty glass tube.

3.2.1 The measurements

In experiments we analyse the compression of the wet state of the hydrogel spheres. For this purpose we have to get an impression of the influences on our measurement time in a normal measurement first. Therefore we measure the deformation of different hydrogel spheres under a constant pressure of 1 N for two of our particle types.

The force versus the deformation is then measured in two ways. The first way is by applying a constant force and increasing it stepwise. The second way is to apply the force only for short times and then end the contact of the sphere to the top piston for some time (in our case we use a relaxation time of 60 seconds). In the first measurement the evaporation has to be taken into account. In the second measurement the evaporation and other fluctuations in the measurement are removed by calculating the weight of the uncompressed sphere after every step.

Last we measure the compression of the sphere on high forces to get a feeling for the limits of Hertzian theory. For this purpose we use the algorithm with relaxation time between the measurements.

3.3 The disc compression setup

3.3.1 The Nanotom

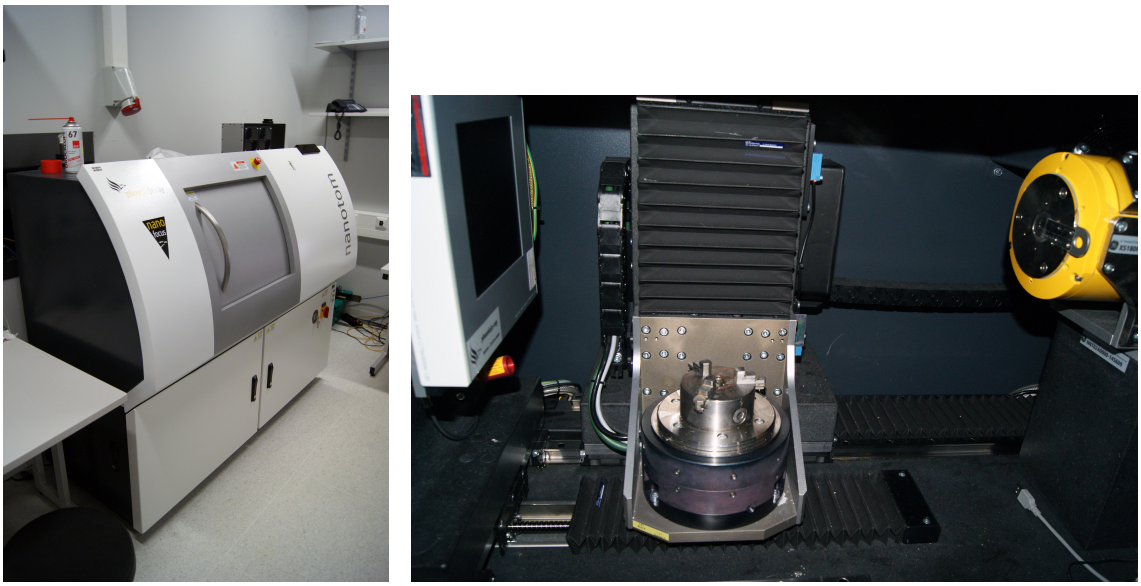

(a) Exterior view.

(b) Interior view. The x-ray Source is on the right and the detector on the left. In the middle is a holder for the samples.

Figure 3.9: The exterior and interior view of the Nanotom, a computer controlled x-ray tomography system.

The Nanotom is a computer controlled tomography system produced by GE Measurement & Control Solutions. We used it here for simple radiogram measurements. The machine consists in principle of a x-ray tube, a sample holder, a detection screen and a safety encapsulation. It can be controlled by a computer. A picture of the machine can be seen in figure 3.9.
Before we were able to start the planned measurements we calibrated the Nanotom with a big PDMS sample in a petri dish. This sample also has a bronze layer in the middle of two PDMS layers. The sample is shown in figure 3.10(a). The resulting radiograms taken with the Nanotom are shown in figure 3.10(b). Through this we get the following calibration values for a radiogram of a PDMS disc with bronze

tracers:

Variable	Value
Voltage	100 kV
Current	100 μA
Shutter-time	500 ms
Averages	20
Skip pictures	4
Binning	(4 x 4) px
Resolution	(2000 x 2000) px

As shown in the pictures with some image processing the bronze particles can be used as tracers for changes in a PDMS disc.

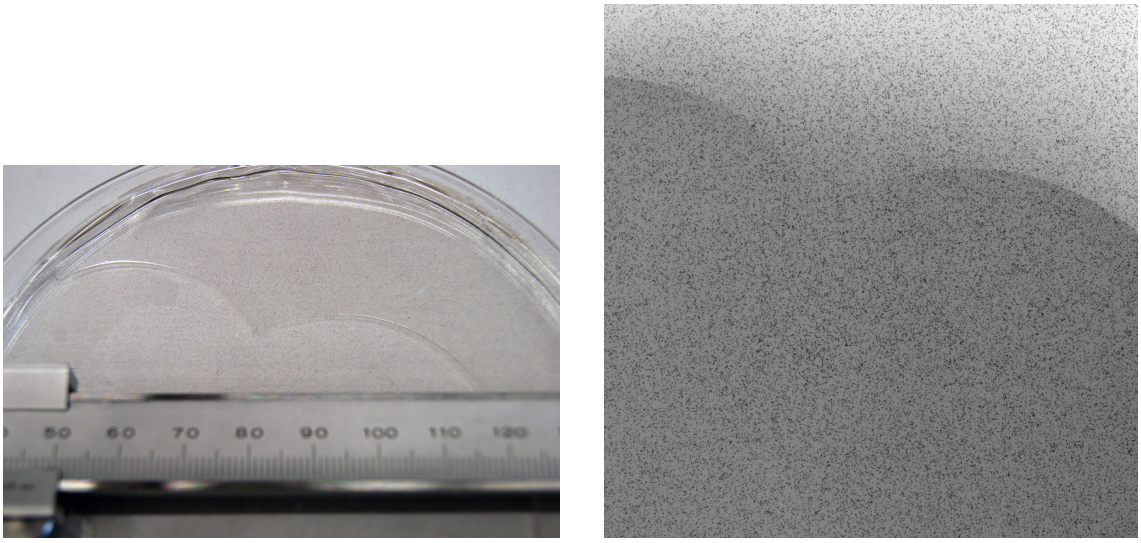

(a) Photography. (b) Radiogram.

Figure 3.10: Photography and radiogram of the PDMS disc to calibrate the Nanotom. The bronze particles are visible in the radiogram and could be used as tracers for further measurements. The curved border visible in both pictures is caused by a thickness change of the PDMS sample.

3.3.2 The sample cell

For the compression of the discs a cell is needed which is able to hold the discs in place and apply force on the discs. The 10 cm x 10 cm cell we wanted to use for this is shown in figure 3.11. The discs are placed at the bottom with a bracket on top. It

is possible to stack several weights on top of the bracket to increase the force. The bracket weighs 50.1 g and the weights weigh 124 g.

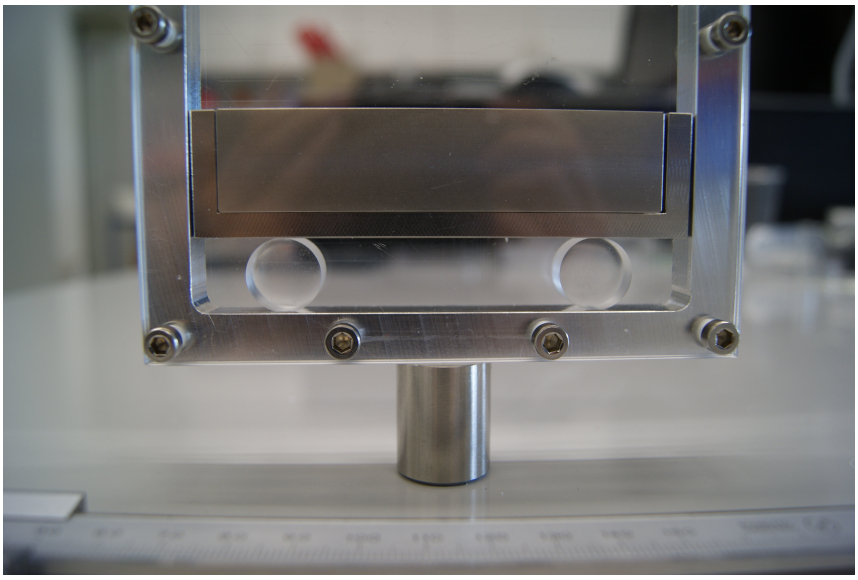

Figure 3.11: The cell designed for the compression of PDMS-discs. The design is meant to be installed in the Nanotom. The pressure on the discs in the middle is applied by weights which can be stacked on a bracket on top of them. In this case only one of the weights is in the bracket. The bracket weighs 50.1 g and each of the weights has a weight of 124 g.

3.3.3 The measurements

It was planned to place the cell in the Nanotom with a single disc without any extra weight on the particle. With the help of the Nanotom a radiogram of the disc is taken. Then the weight on the disc is increased in several steps. Another radiogram is taken for every step. After that the pictures are analysed with a particle image velocimetry (PIV) analysing program. Thereby we planned to get the strain field in the disc by the displacement of the bronze tracers between the unloaded disc and the stressed disc.
Sadly the Nanotom was broken at the time we wanted to take our measurements and could not be repaired till the end of this thesis. Therefore there are no results for the compression of the PDMS discs available for this thesis.

4 Results

Now we want to take a look at the results of our measurements. Sadly this is limited to the results of the measurements of the hydrogel spheres as we couldn't finish the PDMS experiments.

4.1 Time effects in the measurements

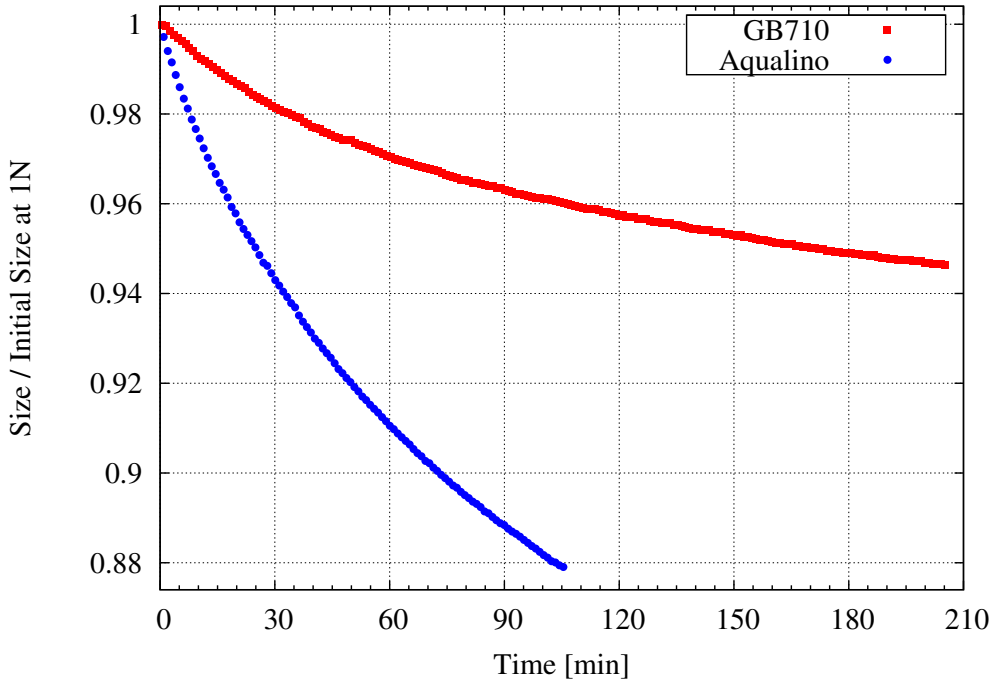

Figure 4.1: Deformation of hydrogel spheres under a constant pressure of 1 N over time. The Aqualinos deform much faster than the GB710 which we have used for all other measurements.

The second time based effect beside the evaporation is the deformation of the hydrogel over time under a certain stress. Figure 4.1 shows two examples for the deformation of hydrogel spheres from different companies. We distinguish them by

the name they were given by the companies. The first type is called Aqualinos and the second type GB710.[1] The Aqualinos are a bit smaller than the GB710 (about 2 mm in the dry state and 12 mm in the wet state).
As it can be seen in the plot the Aqualinos deform faster under stress than the GB710. That's why we decided to use the GB710 for the other experiments. This deformation is the reason for the hysteresis in the following plots. Therefore in contrast to the evaporation it can't be ignored in the experiments. It is an expression of the viscoelastic properties of the hydrogels causing them to deform irreversibly over the time under stress.

4.2 The Hertzian compression of hydrogels

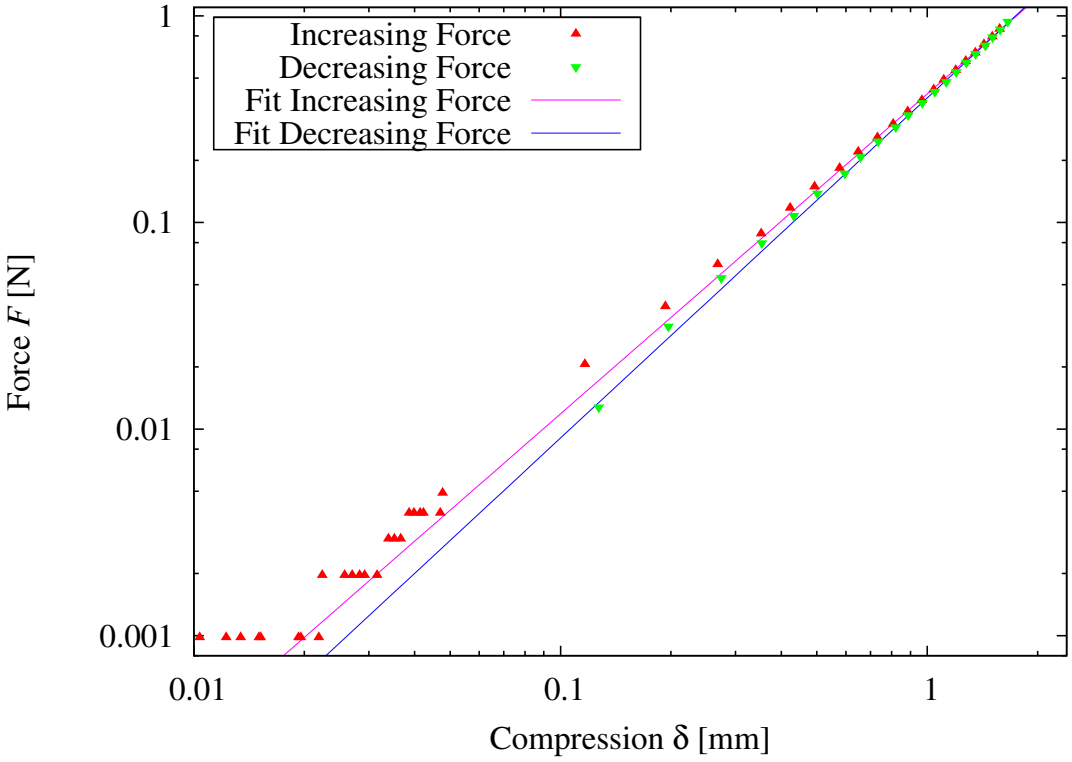

Figure 4.2: Continuous compression δ of a hydrogel sphere. A hysteresis between the increasing force and the decreasing force is visible. The fit parameters can be found in table 4.1.

[1] Aqualinos were disposed by the Zebra Freizeitmöbel und Leitern GmbH and GB710 by Educational Innovations Inc.

Finally we want to take a look at the behaviour of the hydrogel spheres under compression. Therefore we plot the applied force against the compression of the sphere. According to Hertzian theory we expect an exponential behaviour. Within logarithmic scaling this results in a linear relationship. This can be seen in the figures 4.2 and 4.3. In the first plot the continuous application of the force is depcited. The compression is increased stepwise. It is visible that there is a difference between the increasing force and the decreasing force. As mentioned above this hysteresis is a consequence of the viscoelasticity of the particles.
To reduce the effect of the deformation we introduced another algorithm. Between each measurement the hydrogel has time to relax. This can be seen in figure 4.3. The hysteresis is again visible but clearly reduced.

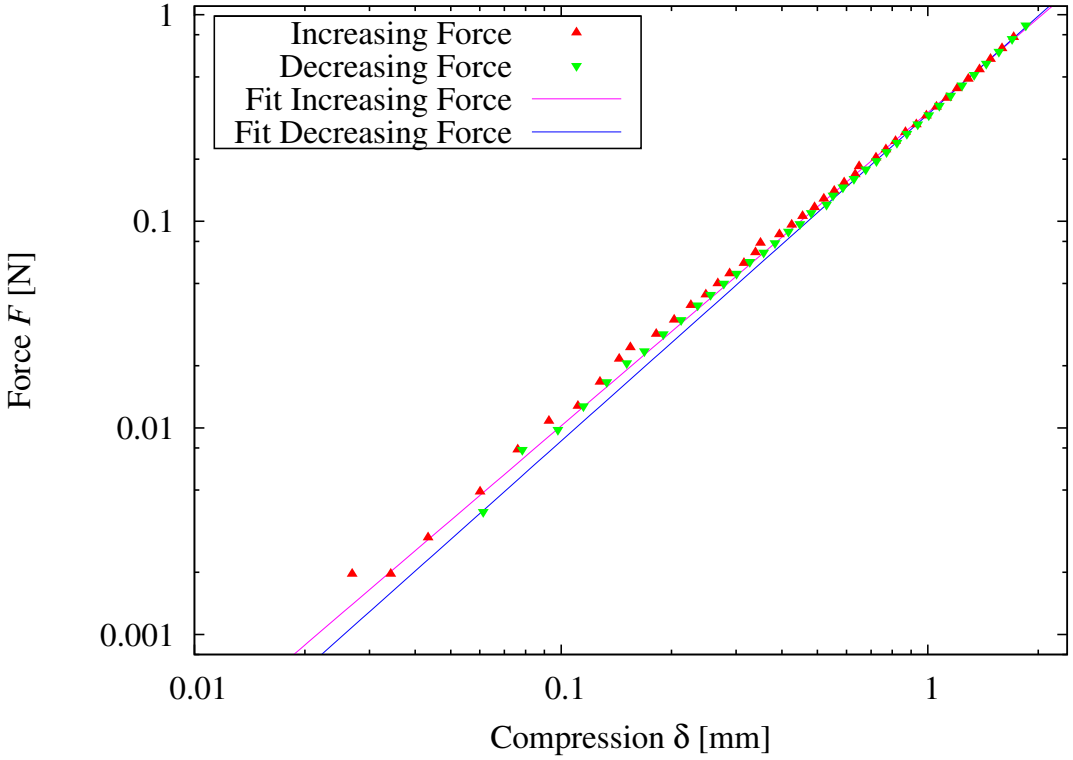

Figure 4.3: Compression δ of a hydrogel sphere with relaxation time between each measurement. The data is divided into the points with increasing force and the ones with decreasing force. Once again the fit parameters can be found in table 4.1.

To quantify this effect we make power function fits on the data. In the case of continuous force application (see figure 4.2) we fit a power function in the form $F(\delta) = a \cdot \delta^b$ on the one hand to the increasing force and on the other hand to the

decreasing force. We also do this for the measurement with relaxation time (see figure 4.3). For fitting we use a χ^2-test with gnuplot. The results from these fits can be seen in table 4.1.

Fit	a [N/mm$^{3/2}$]	b
Continuous increasing force	0.420	1.549
Continuous decreasing force	0.401	1.647
Increasing force with relaxation time	0.336	1.517
Decreasing force with relaxation time	0.329	1.581

Table 4.1: Fit parameters a and b of the Hertzian plots in figures 4.2 and 4.3. The fit function which is used has the form $F(\delta) = a \cdot \delta^b$.

As it can be seen in the table we nearly get the relation $F \propto \delta^{3/2}$ predicted by Hertzian theory. With its help we can calculate the elastic modulus for a known Poisson' ratio. The Hertzian theory (as shown in equation 2.11) implies that the constant of proportionality a is equal to $\sqrt{\frac{8dE^2}{9(1-\nu^2)^2}}$. It follows:

$$E = \sqrt{\frac{9a^2(1-\nu^2)^2}{8d}} \tag{4.1}$$

We use a Poisson's ratio for Polyacrylamid which can be found at [8] as we didn't measured it ourselves. We get a Poisson's ratio of $\nu = 0.457$. The diameter of the particle d is estimated as 18 mm and the exponent b is estimated as 3/2. From this we get the elastic modulus E as depicted in table 4.2.

Fit	E [kPa]
Continuous increasing force	83
Continuous decreasing force	79
Increasing force with relaxation time	66
Decreasing force with relaxation time	65

Table 4.2: Elastic modulus E calculated from the experiments with the help of equation 4.1.

To evaluate our result we compare it with results from other groups. In [9] it was shown that polyacrylamide has a elastic modulus of approximately 70 kPa to 120 kPa depending on the factors like temperature and the production process of the hydrogel. Our results are perfectly within this margin.

4.3 Limitations of Hertzian theory

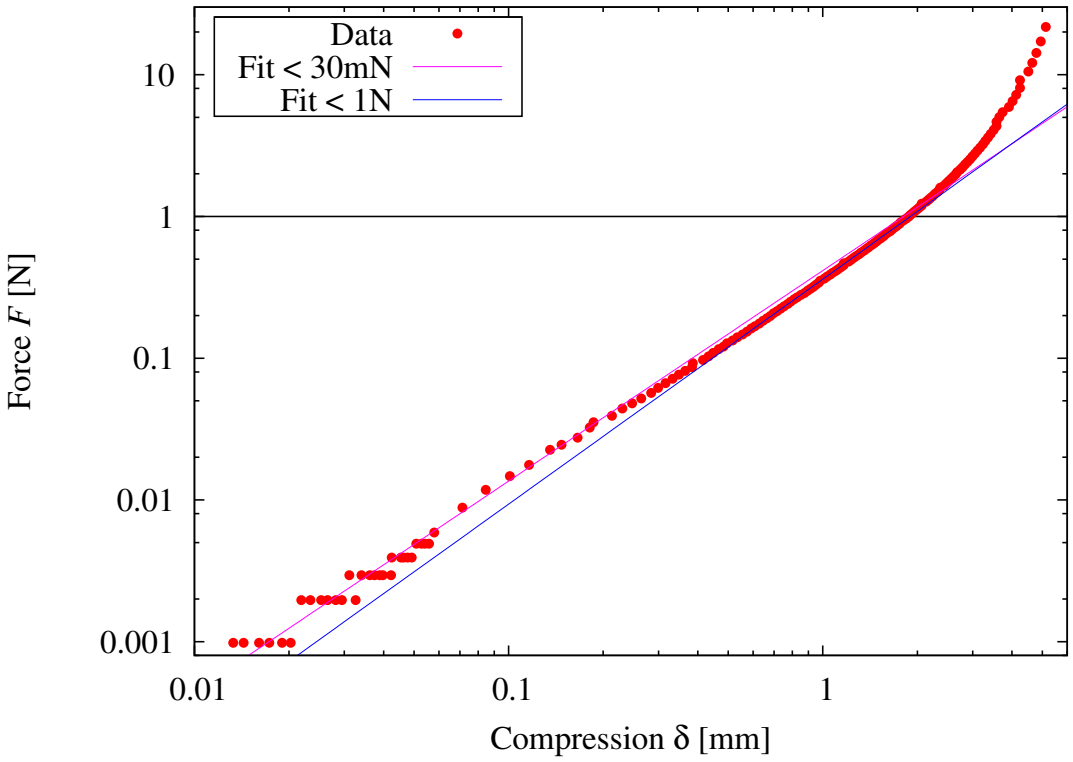

Figure 4.4: Compression δ of a hydrogel sphere with relaxation time between each measurement up to high forces. The fits are both of the form $F(\delta) = a \cdot \delta^b$ and the fit parameters can be found in table 4.3. It is visible that the measured deformation diverges from Hertzian theory for forces >1 N.

Of course the Hertzian theory has its limitations regarding our measurements. As visible in figure 4.4 the compression follows the power fit only up to a force of about 1 N. To make this clearer we calculated the difference between the fits and our data. The results of this are depicted in figure 4.5. The resulting function parameters of the two power fits are presented in table 4.3. The elastic modulus is calculated as described in chapter 4.2.
This shows us that it is reasonable to estimate our data as Hertzian till a maximal force of 1 N. The other problem at higher forces is the irreversible deformation of the hydrogel as described in chapter 4.1. Hence we limited our other experiments only to smaller forces (in the case of this thesis to 0.8 N). With these results we get the limitations for Hertzian theory within our experiments as the resolution of the scale limits the force measurements to at least 1 mN.

Fit	a [N/mm$^{3/2}$]	b	E [kPa]
$<$ 30 mN	0.415	1.485	82
$<$ 1 N	0.361	1.587	71

Table 4.3: Fit parameters a and b of the Fits of figure 4.4. The function which is used has the form $F(\delta) = a \cdot \delta^b$. The elastic modulus E is calculated the same way as in chapter 4.2.

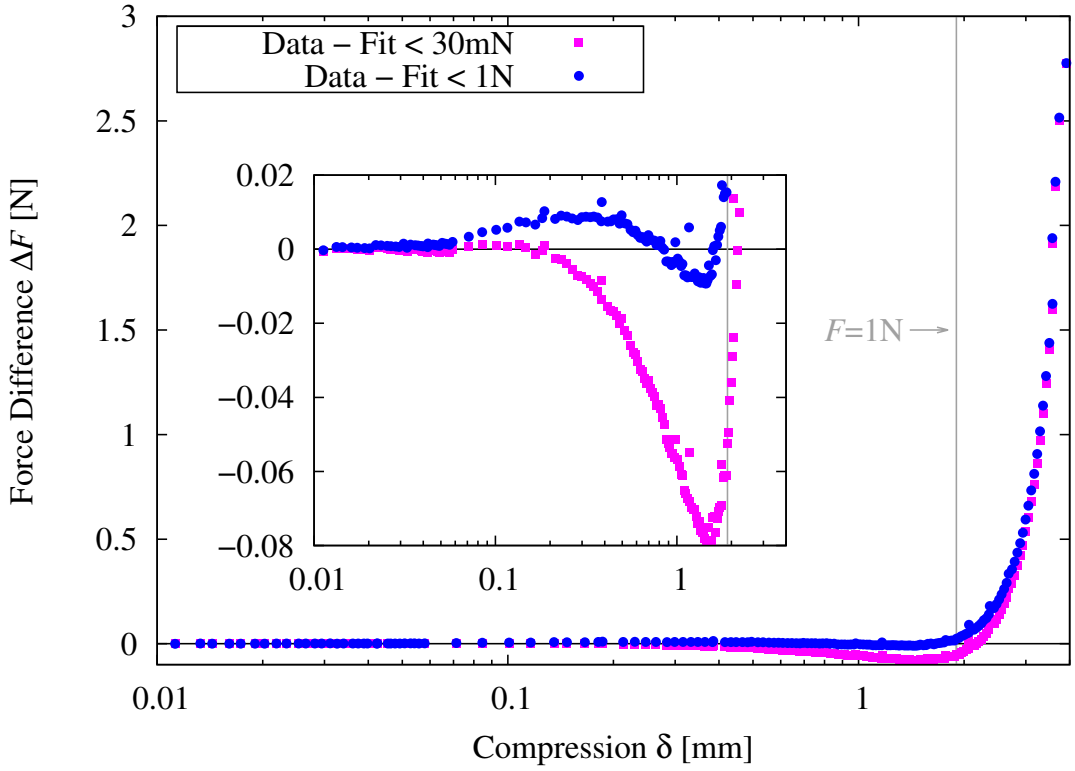

Figure 4.5: Difference between the force in the data and in the fits ΔF for the measurement shown in figure 4.4. The inlay shows the same data on a different force scale. The plots show only the data up to a compression of 4 mm, as the divergence of data only further on higher compressions. The grey line marks the point were the fit "<1 N" reaches 1 N.

5 Conclusion

In this thesis we have shown that our setup is able to measure deformations with good accuracy and that the compression of gels can be described with the help of Hertzian theory.
Regarding our compression setup we have shown that in the measurements different effects have to be taken into account such as capillary bridges, evaporation and deformation of the viscoelastic model bodies. We can also prove that the hydrogels we use indeed behave according to Hertzian theory in the range of two magnitudes of the applied force. In addition to the quality of the fits we got reasonable quantitative evidence for this by the determination of the elastic modulus. Therefore they pose a good model body for these and for further experiments.
Regarding the tests with PDMS it can be said that it seems to be an appropriate material for measurements of the strain field in elastic bodies. Sadly the proof for this is missing due to the technical failure.

5.1 Outlook

First of all obviously we could continue this thesis with the measurements we weren't able to do with the PDMS. It would show us whether the measurement of strain fields by this method can compete with methods like measurements with birefringence and photoelastic materials.
Regarding the hydrogels there are two possible next steps. The first one could be to try to produce the polyacrylamide by ourself to get full control of the particle production. A manual for this can be found at [2]. Furthermore this would give as the chance to use other body-forms. This can help to measure the elastic modulus and the Poisson's ratio, as we could get a known contact area or a measurable change of the body-width. There are other theories to extend Hertzian theory to large compressions (e.g. [10]-[12]). As a second step we can try to check if we can describe the behaviour of the hydrogels with their help. One of the most important

restrictions of Hertzian theory is the limitation on small deformations. This causes a problem with elastic materials as the deformations normally can't be limited only to small deformations.
Additionally it would be an important step to move to more than one particle. The PDMS setup is already suitable for this as a certain amount of discs of the given size fit into the cell. If we find a way to produce the hydrogels by ourselves we would be able to insert tracers in the hydrogels too. Thereby we would be able to take tomograms of packings of elastic spheres and other bodies.
It is planned to at least summarise our current results on the mechanical properties of hydrogels in a proper scientific report.

Bibliography

[1] H. Hertz. Über die Berührung fester elastischer Körper. *Journal für reine und angewandte Mathematik*, 92:156-171, 1882

[2] Margaret L. Byron, Evan A. Variano. Refractive-index-matched hydrogel materials for measuring flow-structure interactions. *Experiments in Fluids*, 54:1456, 2013.

[3] Shomeek Mukhopadhyay and Jorge Peixinho. Packings of deformable spheres. *Physical Review E*, 84:011302, 2011.

[4] Masao Doi. *Soft Matter Physics*, chapter 1.1, 1.5 and 3.4. Oxford University Press, 2013.

[5] Jessamine Ng Lee et al. Solvent Compatibility of Poly(dimethylsiloxane)-Based Microfluidic Devices. *Analytical Chemistry*, 75:6544-6554, 2003

[6] K.L. Johnson. *Contact Mechanics*, chapter 4. Cambridge University Press, 1985.

[7] Hans-Jürgen Butt, Michael Kappl. Normal capillary forces. *Advances in Colloid and Interface Science*, 146:48-60, 2009.

[8] T. Takigawa et al. Possion's ratio of polyacrylamide (PAAm) gels. *Polymer Gels and Networks*, 4:1-5, 1996.

[9] E.C. Muniz, G. Geuskens. Compressive Elastic Modulus of Polyacrylamide Hydrogels and Semi-IPNs with Poly(N-isopropylacrylamide). *Macromolecules*, 34:4480-4484, 2001.

[10] Y.Tatara. Extensive Theory of Force Approach Relations of Elastic Spheres in Compression and in Impact. *Journal of Engineering Materials and Technology*, 111:163-168, 1989

[11] Y.Tatara. On Compression of Rubber Elastic Sphere Over a Large Range of Displacements. *Journal of Engineering Materials and Technology*, 113:285-295, 1991.

[12] K. K. Liu et al. The large deformation of a single micro-elastic sphere. *Journal of Physics D: Applied Physics*, 31:294-303

Acknowledgements

I would like to thank everyone who helped me to complete this thesis. First of all, I would like to thank Dr. Matthias Schröter for supervising my work and to be my first referee for this work. He provided help and guidance whenever needed during this project. Second I would like to thank Prof. Dr. Sarah Köster who kindly agreed to be my second referee for this thesis.
Further I would like to express my gratitude for Stefan Winter and Caroline Campbell who were my proof-readers for this thesis. In addition I would like to thank Caroline Bauer for her help with the organization and care of the plants needed for our measurements. I also would like to thank Wolf Keiderling, Birte Riechers and Markus Benderoth for their support in designing and producing the setups and materials.
Lastly I would like to thank the Max-Planck-Institute for Dynamics and Self-Organization and the Botanical Garden in Göttingen for providing me with the materials and laboratories needed for this project.

Erklärung nach §13(8) der Prüfungsordnung für den Bachelor-Studiengang Physik und den Master-Studiengang Physik an der Universität Göttingen:

Hiermit erkläre ich, dass ich diese Abschlussarbeit selbständig verfasst habe, keine anderen als die angegebenen Quellen und Hilfsmittel benutzt habe und alle Stellen, die wörtlich oder sinngemäß aus veröffentlichten Schriften entnommen wurden, als solche kenntlich gemacht habe.
Darüberhinaus erkläre ich, dass diese Abschlussarbeit nicht, auch nicht auszugsweise, im Rahmen einer nichtbestandenen Prüfung an dieser oder einer anderen Hochschule eingereicht wurde.

Göttingen, den 8. Juli 2014

(Markus Richter)